Supporting Information

Purposely constructing direct Z-scheme photocatalyst by photo-deposition technique

Wenshuai Jiang, [a] Dan Qu,*[a] Li An, [a] Xiang Gao, [a] Yuanjing Wen, [a] Xiayan Wang, [a] Zaicheng Sun*[a]

a. Center of Excellence for Environmental Safety and Biological Effects, Beijing Key Laboratory for Green Catalysis and Separation, Department of Chemistry and Chemical Engineering, College of Environmental and Energy Engineering, Beijing University of Technology, Beijing, 100124, P. R. China.

Email：sunzc@bjut.edu.cn and danqu@bjut.edu.cn

Content

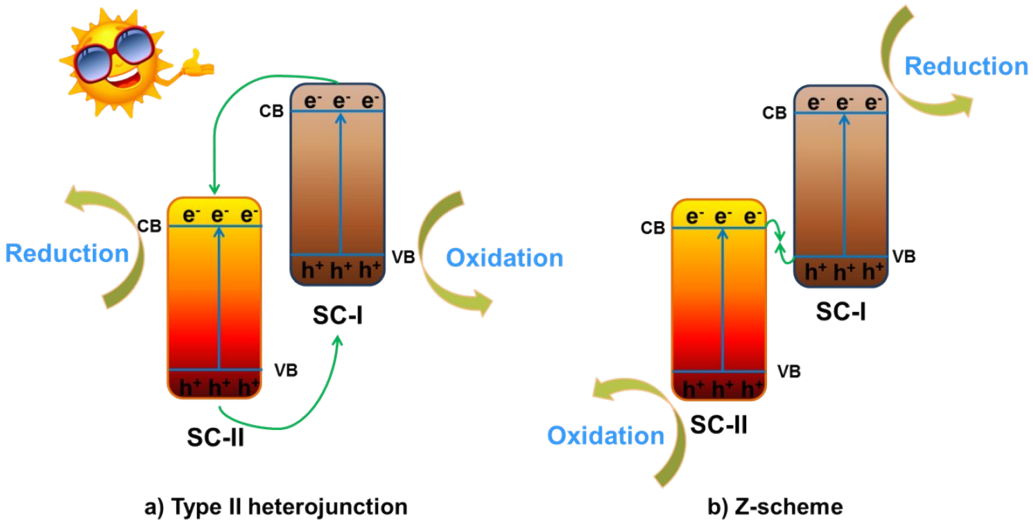

Scheme S1. Schematic of the charge-carrier separation and mechanism on the type II heterojunction (a) and the direct Z-scheme (b) composed with two different semiconductors (SC-I and SC-II).

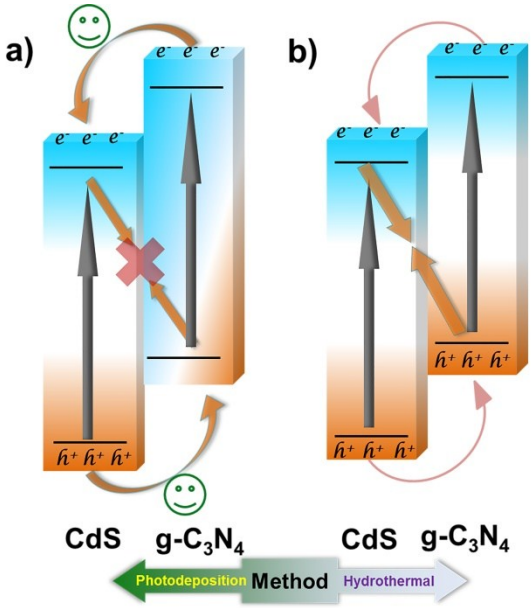

Scheme S2. Schematic of the charge-carrier separation and mechanism of g-C_3N_4/CdS composites synthesized by the methods of photodeposition (a) and hydrothermal (b), respectively.[1]

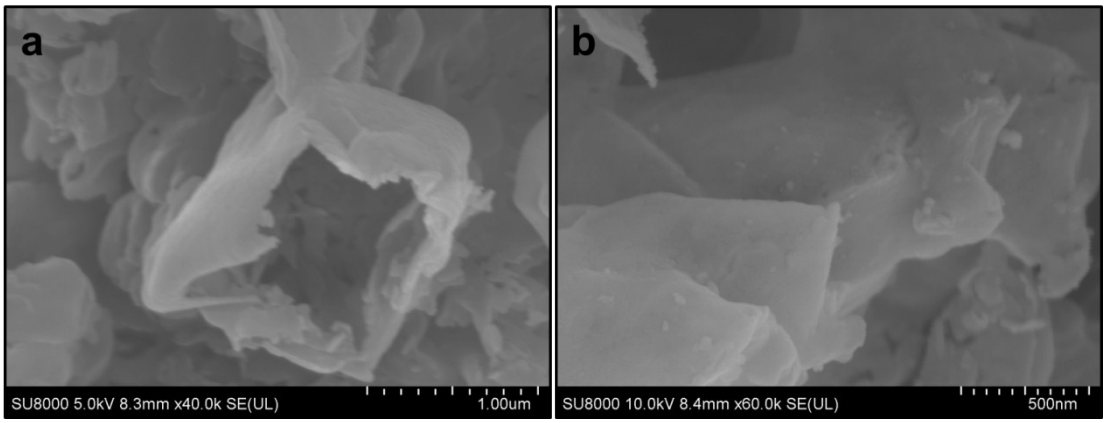

Fig. S1. The SEM of g-C_3N_4 nanosheets (a) and 5%-FCN (b)

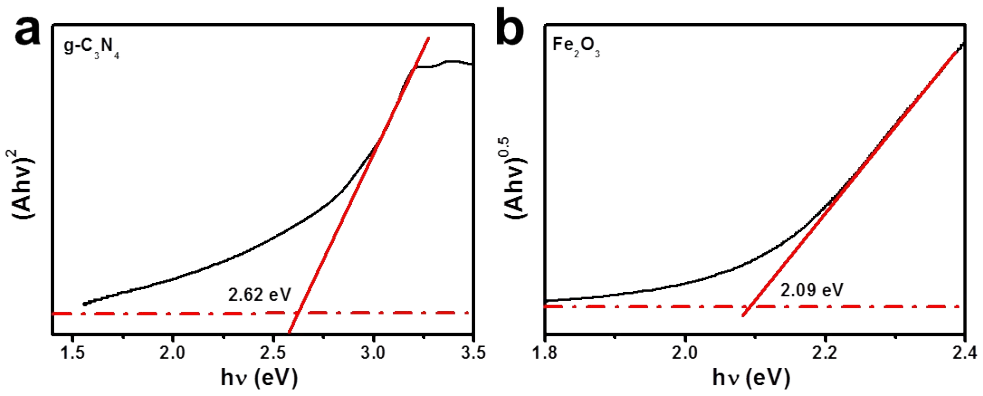

Fig. S2. Tauc-plot of the $(Ahv)^2$ versus hv for g-C_3N_4 (a) and the $(Ahv)^{0.5}$ versus hv for Fe_2O_3 (b).

In general, the band edge positions of CB and VB of a semiconductor can be determined using Tauc-plot method.[2] The conduction band (CB) edge of a semiconductor at zero charge can be determined using the following equation:

$$E_{CB} = \chi - E^e - 1/2E_g \quad (1)$$

$$E_{VB} = E_g + E_{CB} \quad (2)$$

Where, E_{CB} is the CB edge potential, E_{VB} is the valance band (VB) edge potential, and χ is the electronegativity of the semiconductor, expressed as the geometric mean of the absolute electronegativity of the constituent atoms, which is defined as the arithmetic mean of the atomic electron affinity and the first ionization energy. E^e is the energy of free electrons on the hydrogen scale ≈4.5 eV and E_g is the band gap of the semiconductor.

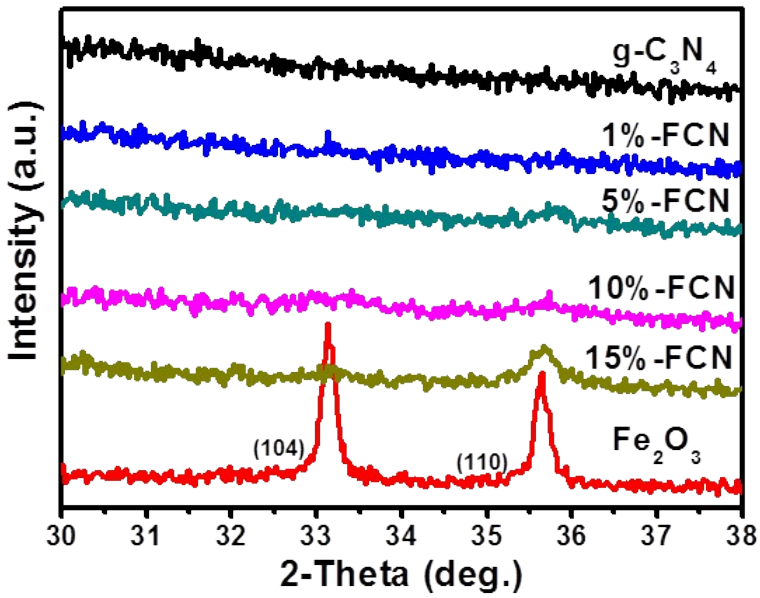

Fig. S3. The XRD patterns of g-C_3N_4, Fe_2O_3 and x%-FCN samples.

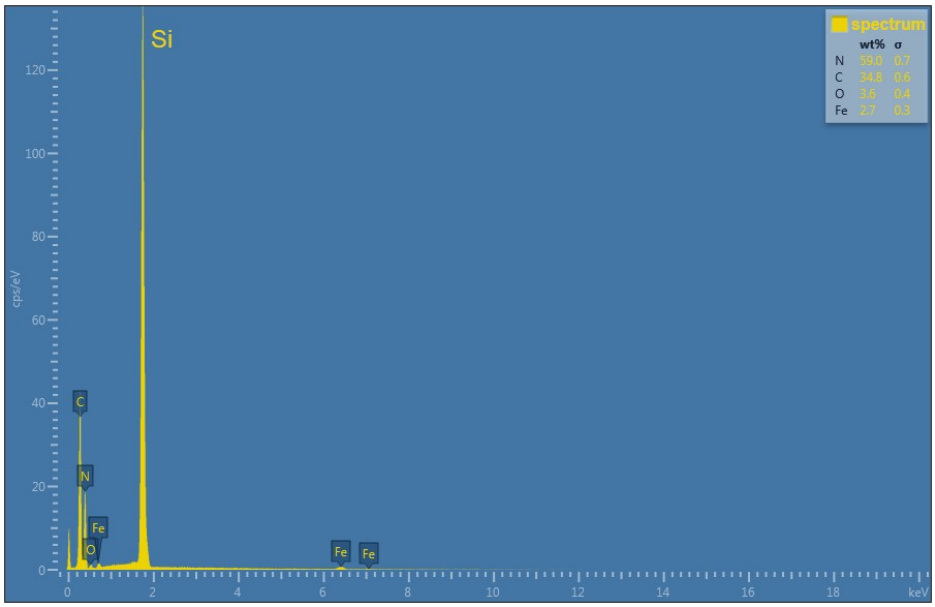

Fig. S4. The EDS spectrum of 5%-FCN

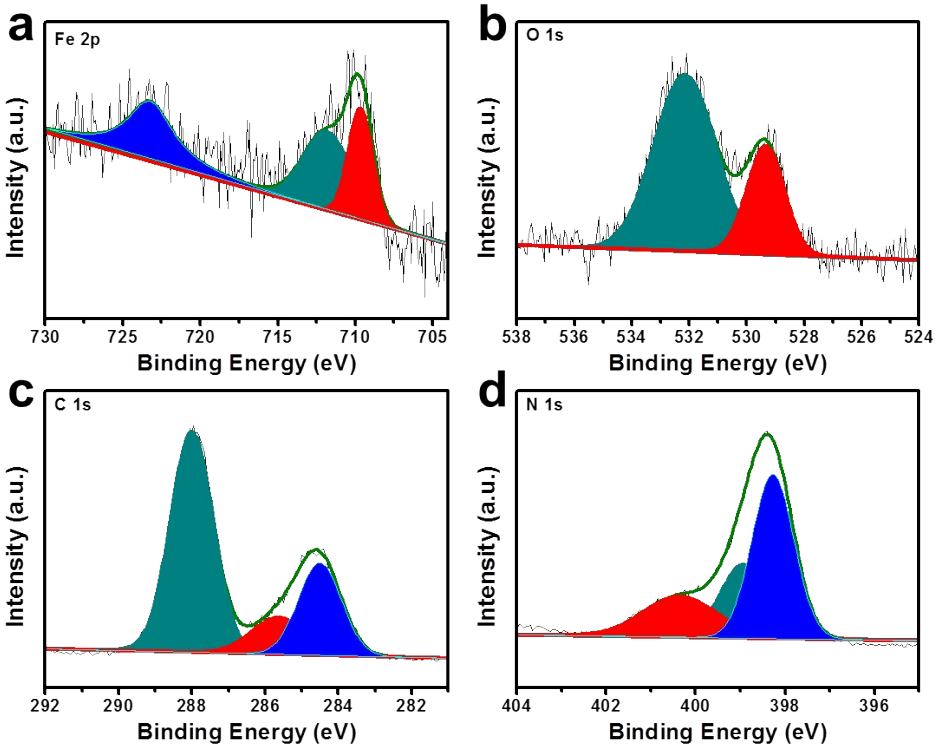

Fig. S5. XPS high-resolution spectrum of (a) Fe 2p, (b) O 1s, (c) C 1s, (d) N 1s of the 5%-FCN.

To further prove the composition of the complex are Fe_2O_3 and g-C_3N_4, high-resolution XPS spectra (Fig. S5) of N 1s, Fe 2p, and O 1s in the 5%-FCN were investigated. For the N1s spectrum, the peak can be break up into three peaks at 398.4, 398.9, and 400.5 eV, which can be ascribed to the occurrence of C-N=C groups, tertiary nitrogen N-$(C)_3$ groups, and N-H groups. Fe 2p exhibits two obvious peaks at 711.0 and 712.5, 724.5 eV, which correspond to Fe 2p3/2, Fe 2p3/2and Fe 2p1/2, respectively. The high-resolution spectrum of O 1s shows a peak at 529.9 eV, which is attributed to the lattice oxygen, and a peak at 532.6 eV, which is assigned to oxygen-containing intermediates derived from the incomplete thermal condensation of urea.

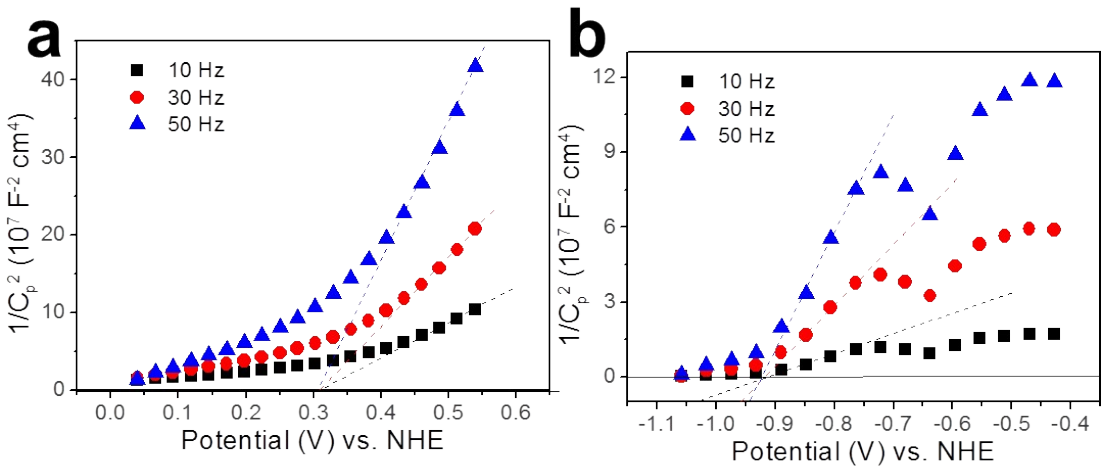

Fig. S6. Mott-schottky curve of Fe_2O_3 (a) and g-C_3N_4 (b)

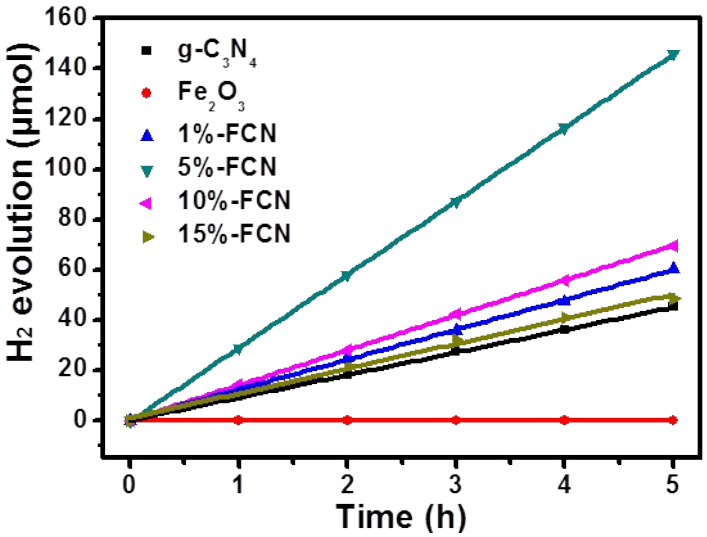

Fig. S7. The amount of H_2 evolution with the x%-FCN samples, g-C_3N_4 and Fe_2O_3 under visible light ($\lambda > 420$ nm) with 50mg catalysts.

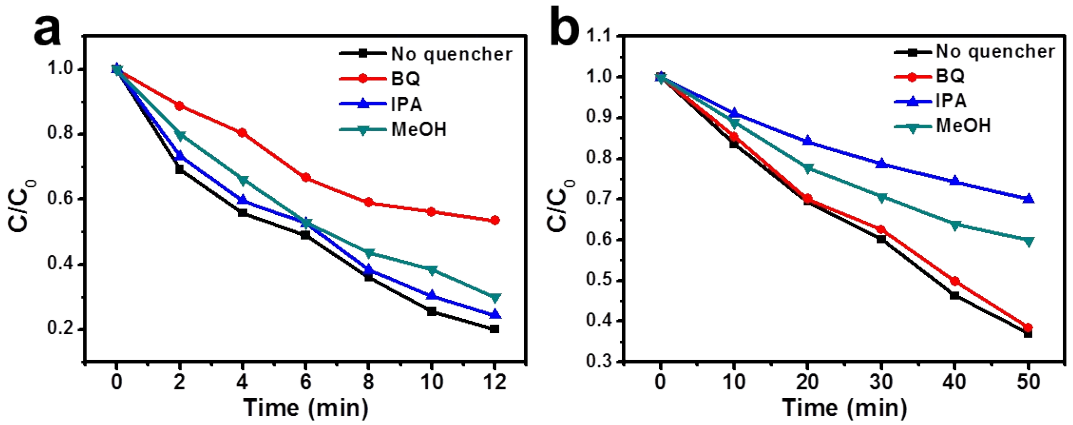

Fig. S8. Photocatalytic degradation of RhB aqueous solution over g-C_3N_4 (a) and Fe_2O_3 (b).

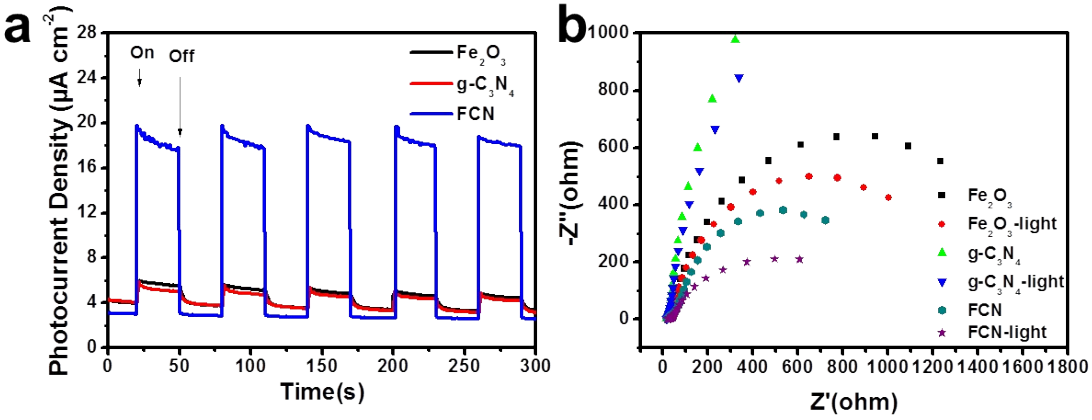

Fig. S9. (a). Transient photocurrents meansurement of the g-C_3N_4, Fe_2O_3 and 5%-FCN samples; (b) Electrochemical impedance spectroscopy (EIS) of g-C_3N_4, Fe_2O_3 and 5%-FCN with/without light irradiation.

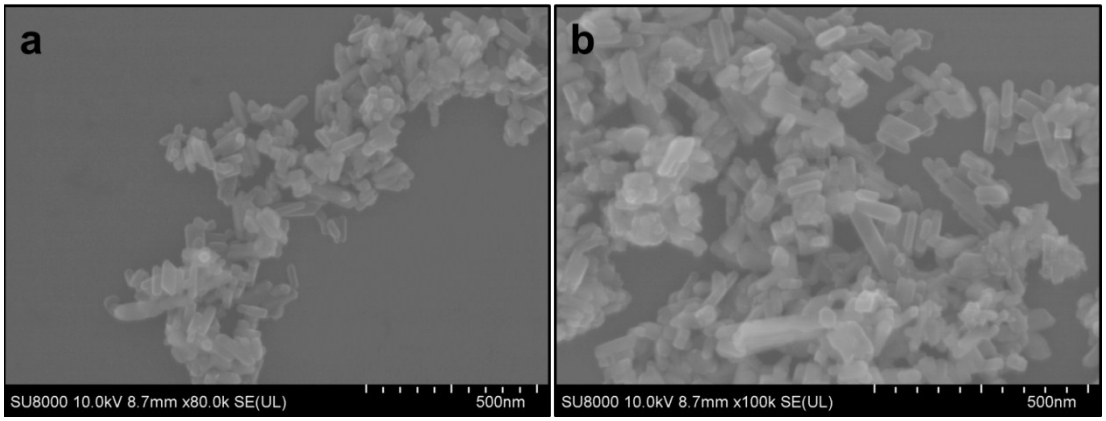

Fig. S10. The SEM of TiO_2 (a) and CdS/TiO_2 (b)

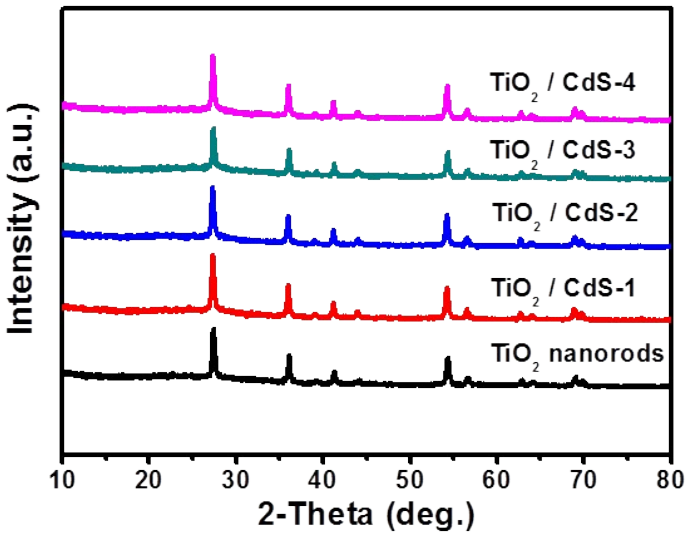

Fig. S11. The XRD of TiO_2 nanorods and CdS/TiO_2 samples

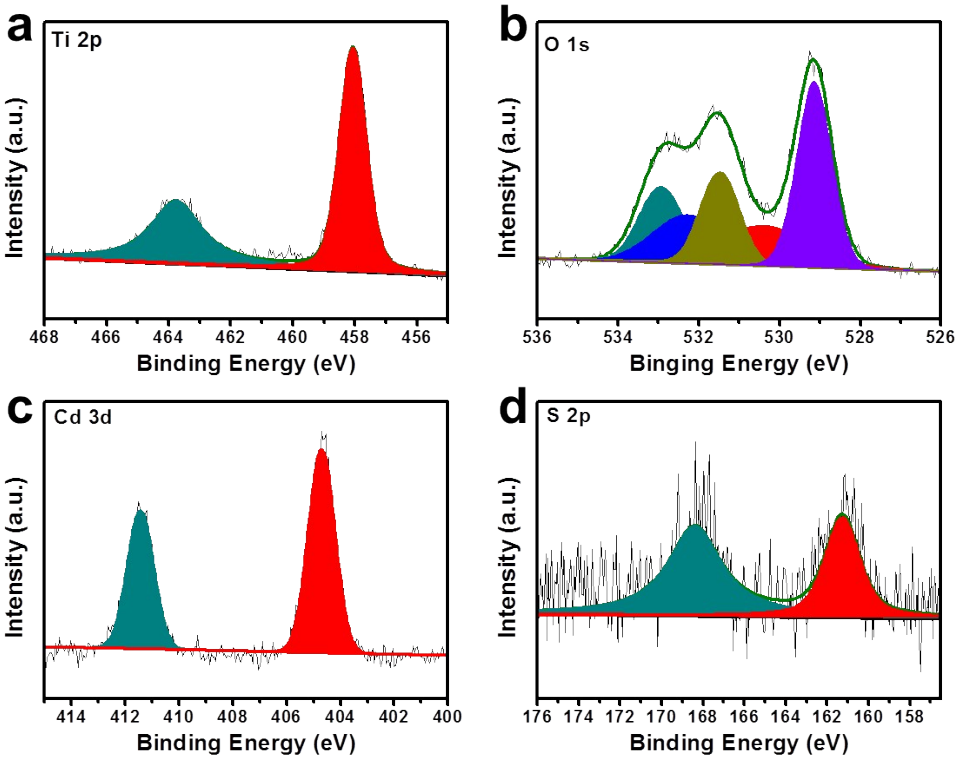

Fig. S12. XPS high-resolution spectrum of (a) Ti 2p, (b) O 1s, (c) Cd 3d, (d) S 2p of the CdS/TiO_2.

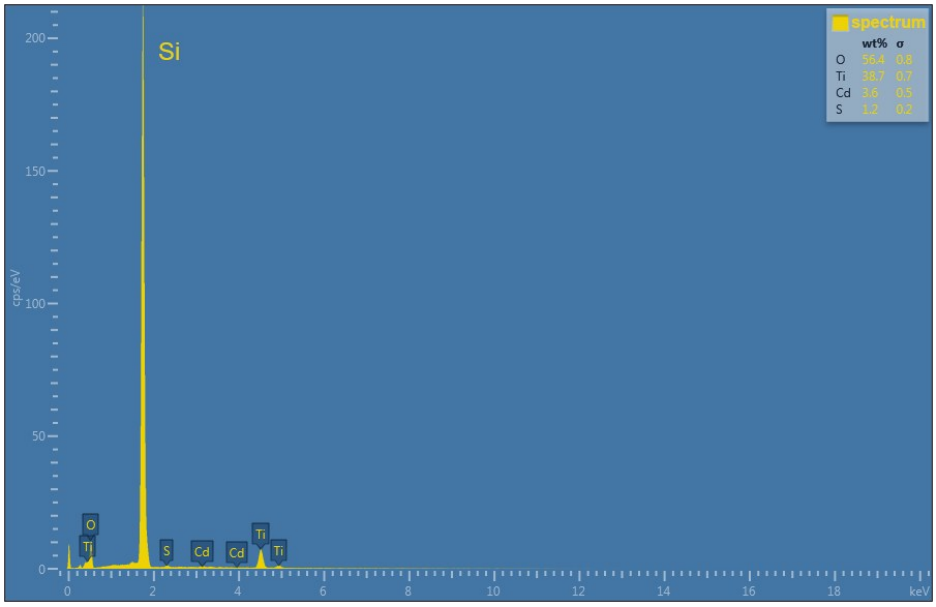

Fig. S13. The EDS spectrum of CdS/TiO_2-3

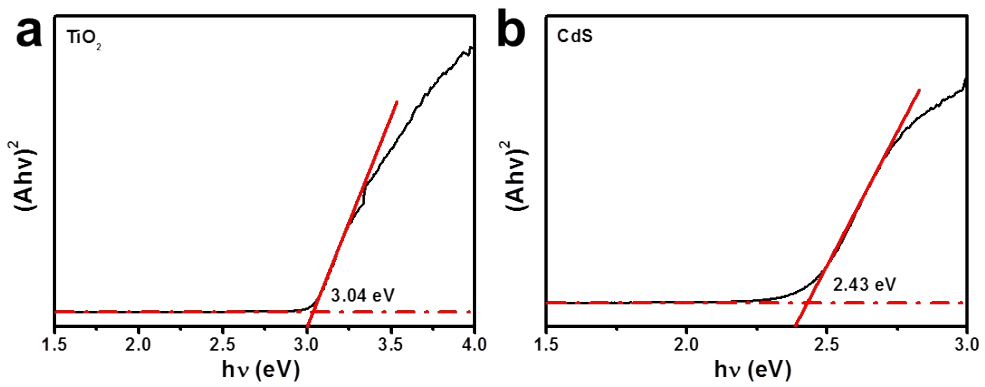

Fig. S14. Tauc-plot of the $(Ahv)^2$ versus hv for TiO_2 (a) and CdS (b).

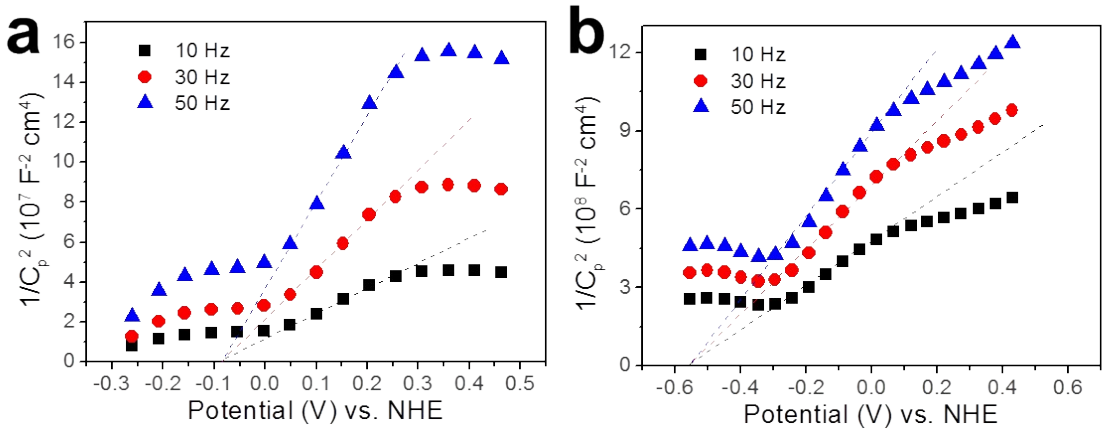

Fig. S15. Mott-schottky curve of TiO_2 (a) and CdS (b)

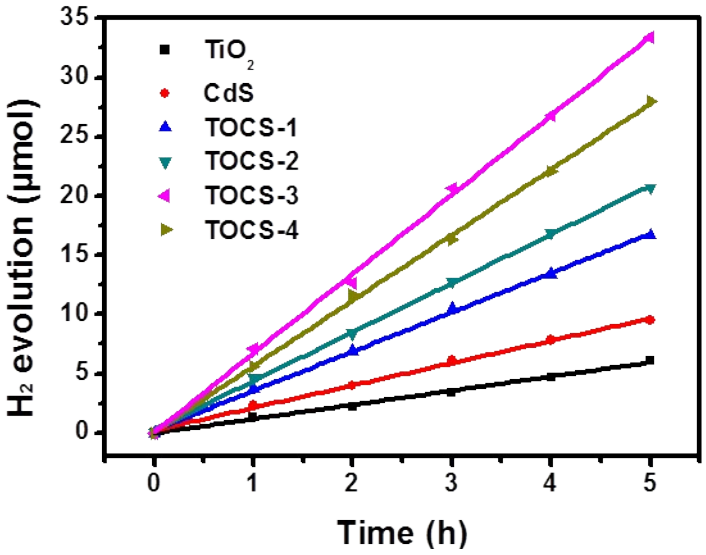

Fig. S16. The amount of H_2 evolution with the CdS/TiO_2 samples, TiO_2 and CdS under the light of $\lambda > 400$ nm

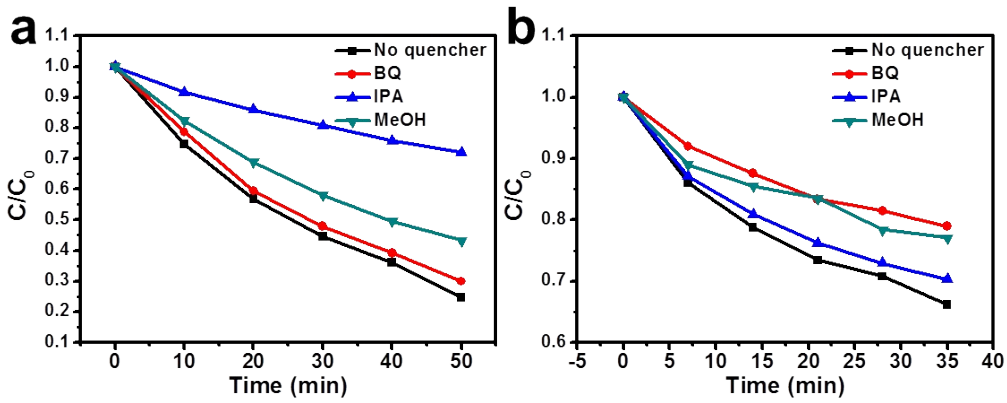

Fig. S17. Photocatalytic degradation of RhB aqueous solution by TiO_2 (a) and CdS (b).

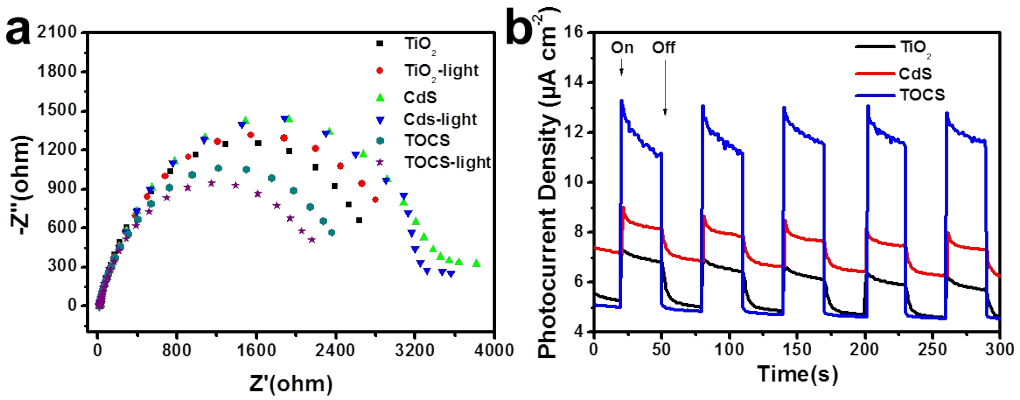

Fig. S18. (a). Transient photocurrents meansurement of the TiO_2, CdS and CdS/TiO_2-3 samples; (b) Electrochemical impedance spectroscopy (EIS) of the TiO_2, CdS and CdS/TiO_2-3 with/without light irradiation.

Table S1. Summary of representative direct Z-scheme photocatalysts in water splitting

Summary of representative direct Z-scheme photocatalysts in water splitting						
Catalyst	**Co-catalyst**	**Synthesis method**	**Photocatalytic reaction conditions**	**Products and activity**	**AQE (%)**	**Refs**
Anatase TiO_2/rutile TiO_2	0.6 wt% Pt	Electrospinning and calcination	350 W Xe lamp, methanol solution	H_2: 324 μmol h^{-1}	20.9% (365 nm)	3
TiO_2/WO_3	0.45 wt% Pt	Electrospinning	300 W Xe lamp, methanol solution	H_2: 128.66 μmol h^{-1} g^{-1}		4
TiO_2/WO_3	0.45 wt% Au	Electrospinning	300 W Xe lamp, methanol solution	H_2: 296.63 μmol h^{-1}		5
$ZnO_{1-x}/Zn_{0.2}Cd_{0.8}S$	0.1 wt% Pd	Solid-state synthesis	300 W Xe lamp, λ > 420 nm, 0.1 M Na_2S and 0.1 M Na_2SO_3	H_2: 3779 μmol h^{-1}	62.1% (420 nm)	6
g-C_3N_4/WO_3	3 wt% Pt	Solid-state synthesis	300 W Xe lamp, λ > 420 nm, triethanolamine solution	H_2: 326 μmol h^{-1}	3.9% (420 nm)	7
g-C_3N_4/WO_3	2 wt% Pt	Solid-state synthesis	300 W Xe lamp, λ > 420 nm, triethanolamine solution	H_2: 66 μmol h^{-1} g^{-1}	0.9% (405 nm)	8
$W_{18}O_{49}$/g-C_3N_4	3 wt% Pt	Hydrothermal	300 W Xe lamp, λ > 420 nm, triethanolamine solution	3.69 μmol h^{-1}	1.79% (400 nm)	9
$W_{18}O_{49}$/g-C_3N_4	1 wt% Pt	Solvothermal	300 W Xe lamp, solar filter (AM 1.5), triethanolamine solution	15.2 μmol h^{-1}		10
CdS/SiC	3 wt% Pt	Deposition-precipitation	300 W Xe lamp, λ > 420 nm, 0.1 M Na_2S and 0.1 M Na_2SO_3	H_2: 5460 μmol h^{-1} g^{-1}	2.1% (420 nm)	11
CdS/SiC	No	Hydrothermal	300 W Xe lamp, λ > 420 nm, 0.1 Na_2S and 0.1 M Na_2SO_3	H_2: 363 μmol h^{-1} g^{-1}		12

$CoTiO_3$/g-C_3N_4	3 wt% Pt	Solid-state synthesis	300 W Xe lamp, λ > 400 nm, ethanol solution	H_2: 858 μmol h^{-1} g^{-1}	38.4% at 350 nm, 3.23% at 420 nm	13
Rh doped $SrTiO_3$/$BiVO_4$	0.7 wt% Ru	Solid-state synthesis	300 W Xe lamp, 400 nm < λ < 800 nm, pure water	H_2: 47.2 μmol h^{-1} O_2: 22.4 μmol h^{-1}	1.6% (420 nm)	14
Black phosphorus/$BiVO_4$	5 wt% Co_3O_4	Self-assembly	320 W Xenon lamp, λ > 420 nm, pure water	H_2: 160 μmol h^{-1} O_2: 102 μmol h^{-1}	0.89% (420 nm)	15
TiO_2/CdS	1 wt% Pt	Photoreduction-deposition	300 W Xe lamp, λ > 400 nm, 20 vol% methanol aqueous solution	H_2: 133.6 μmol g^{-1} h^{-1}	3.2 % (400 nm)	Our work
Fe_2O_3/g-C_3N_4	1 wt% Pt	Photooxidation-deposition	300 W Xe lamp, λ > 420 nm, 10 vol% triethanolamine solution	H_2: 584 μmol g^{-1} h^{-1}	17% (380 nm)	Our work

References

1. W. Jiang, X. Zong, L. An, S. Hua, X. Miao, S. Luan, Y. Wen, F. F. Tao and Z. Sun, *ACS Catal.*, 2018, **8**, 2209-2217.
2. J. Jin, J. Yu, D. Guo, C. Cui and W. Ho, *Small*, 2015, **11**, 5262-5271.
3. F. Xu, W. Xiao, B. Cheng and J. Yu, *Int. J. Hydrogen Energ.*, 2014, **39**, 15394-15402.
4. H. Gao, P. Zhang, J. Hu, J. Pan, J. Fan and G. Shao, *Appl. Surf. Sci.*, 2017, **391**, 211-217.
5. H. Gao, P. Zhang, J. Zhao, Y. Zhang, J. Hu and G. Shao, *Appl. Catal. B: Environ.*, 2017, **210**, 297-305.
6. H.-L. Guo, H. Du, Y.-F. Jiang, N. Jiang, C.-C. Shen, X. Zhou, Y.-N. Liu and A.-W. Xu, *J. Phys. Chem. C*, 2017, **121**, 107-114.
7. K. Kailasam, A. Fischer, G. Zhang, J. Zhang, M. Schwarze, M. Schröder, X. Wang, R. Schomäcker and A. Thomas, *ChemSusChem*, 2015, **8**, 1404-1410.
8. H. Katsumata, Y. Tachi, T. Suzuki and S. Kaneco, *RSC Adv.*, 2014, **4**, 21405-21409.
9. K. Song, F. Xiao, L. Zhang, F. Yue, X. Liang, J. Wang and X. Su, *J. Mol. Catal. A: Chem.*, 2016, **418-419**, 95-102.
10. Z. Zhang, J. Huang, Y. Fang, M. Zhang, K. Liu and B. Dong, *Adv. Mater.*, 2017, **29**, 1606688.
11. Y. Peng, Z. Guo, J. Yang, D. Wang and W. Yuan, *J. Mater. Chem. A*, 2014, **2**, 6296-6300.
12. Y. Peng, Z. Guo, D. Wang, N. Pan and W. Yuan, *Appl. Phys. Lett.*, 2015, **107**, 012102.
13. R. Ye, H. Fang, Y.-Z. Zheng, N. Li, Y. Wang and X. Tao, *ACS Appl. Mater. & Inter.*, 2016, **8**, 13879-13889.
14. Q. Jia, A. Iwase and A. Kudo, *Chem. Sci.*, 2014, **5**, 1513-1519.
15. M. Zhu, Z. Sun, M. Fujitsuka and T. Majima, *Angew. Chem. Int. Edit.*, 2018, **57**, 2160-2164.